

Electron-positron outflows from gamma-ray emitting accretion discs

A. M. Beloborodov*

Stockholm Observatory, S-133 36 Saltsjöbaden, Sweden

Accepted, Received

ABSTRACT

An e^\pm atmosphere is inevitably created around a black hole accretion disc, the spectrum of which extends to MeV energies. Pairs created in $\gamma - \gamma$ collisions outside the disc are blown away by soft radiation (which dominates the bolometric luminosity of the disc) and form a semi-relativistic outflow. We simulate numerically the conversion of the MeV radiation into a vertical e^\pm outflow above a disc-like source. The outflowing e^\pm plasma becomes optically thick to Thomson scattering if the compactness of the γ -ray source exceeds ~ 30 . The scattering by e^\pm then collimates the bulk of soft radiation along the disc axis, and the apparent bolometric luminosity of the disc depends strongly on its inclination to the line of sight. The anisotropic central emission may account for the lack of Fe $K\alpha$ lines in the X-ray spectra of bright radio-quiet quasars. The scattering in e^\pm outflows may also explain the orientation of optical polarization in non-blazar active galactic nuclei.

Key words: accretion, accretion discs – black hole physics – plasmas – radiative transfer – gamma-rays: theory

1 INTRODUCTION

The X-ray activity of galactic black hole candidates (GBHs) and active galactic nuclei (AGNs) is usually attributed to accretion discs surrounding putative black holes. A special feature of accreting black holes is that their radiation spectra extend up to the γ -ray band. The γ -rays are thought to be produced in the innermost region of the accretion disc (see, e.g., Svensson 1996 for a review). It may be a cold disc covered by an active corona in which particles are accelerated in magnetic reconnection events (Galeev, Rosner & Vaiana 1979). It may also be a hot two-temperature disc as proposed by Shapiro, Lightman & Eardley (1976).

As soon as the radiation spectrum extends above the electron rest-mass energy, $m_e c^2 = 511$ keV, the reaction $\gamma + \gamma \rightarrow e^- + e^+$ becomes inevitable and leads to production of an electron-positron atmosphere of the black hole (Herterich 1974). Guilbert, Fabian & Rees (1983) showed that if the γ -ray luminosity exceeds $\sim 10^{-3}$ of the Eddington limit for the black hole, the e^\pm atmosphere becomes optically thick to Thomson scattering. The brightest accretion discs thus can be surrounded by optically thick e^\pm envelopes. The dynamics of an e^\pm envelope around a compact γ -ray source has been discussed in various contexts (e.g., Katz 1982; Zdziarski 1984; Guilbert & Stepney 1985; Coppi & Lamb 1992; Illarionov & Krolik 1996; Li & Liang 1996), and it has been shown that the pairs should share the momentum of radiation and form an outflow from the source.

In this paper, we study the formation of vertical e^\pm outflows

from disc-like γ -ray sources. Following the observed spectra of non-blazar AGNs and GBHs, we assume that the γ -rays contribute only a small fraction, $\lesssim 0.1$, to the bolometric luminosity, and the bulk of disc emission is in UV or X-ray bands. The created pairs then move in the dense soft radiation field which forces them to acquire an equilibrium velocity $\sim c/2$ such that the effective radiation pressure acting on the pairs vanishes (Gurevich & Rumyantsev 1965). The equilibrium velocity is determined by the angular distribution of the radiation and can easily be calculated for an optically thin atmosphere. In the optically thick case, the problem becomes non-linear as scattering by moving pairs affects the angular distribution of the radiation above the disc. The corresponding transfer problem can be solved self-consistently to yield both the plasma velocity and radiation intensity as a function of optical depth in the e^\pm atmosphere (see Section 4).

The density of the outflow is governed by pair injection due to $\gamma - \gamma$ interactions. We assume that the primary spectrum of γ -rays emerging from the source has a break at a few MeV due to strong absorption of more energetic photons inside the source. The bulk of $\gamma - \gamma$ interactions outside the disc occur between MeV photons, just above the threshold. The γ -ray transfer is therefore non-linear as the $\gamma - \gamma$ opacity at each height is determined by the MeV radiation field itself. To study the non-linear transformation of γ -rays into an e^\pm outflow, we have developed a code which calculates the hard X/ γ -ray transfer in a slab geometry. Besides the $\gamma - \gamma$ reaction, the code approximately accounts for Compton scattering and annihilation emission of the created pairs, assuming that the pairs move with the typical velocity $v = c/2$.

The main properties of the atmosphere, such as Thomson optical depth and the power of e^\pm outflow, are determined basically by

* Also at Astro Space Centre of Lebedev Physical Institute, 84/32 Profsojuznaja Street, Moscow 117810, Russia

one parameter of the source – the compactness parameter defined in Section 2.1. The results are weakly dependent on the specific internal boundary conditions for the transfer problem. In our calculations, the primary source is simulated in the simplest way: A homogeneous disc emitting hard photons isotropically with a power-law spectrum around 511 keV.

In Section 2, we discuss a general constraint imposed by $\gamma - \gamma$ absorption on the spectrum of an accretion disc. Then, in Section 3, we calculate the rate of pair injection above the disk surface and discuss the formation of an optically thin e^\pm outflow. In Section 4, we consider γ -ray sources with large compactness parameters, which are surrounded by optically thick e^\pm atmospheres, and calculate the e^\pm density and velocity profiles of the optically thick outflows. We also discuss pair acceleration at large distances from the source. The main conclusions are summarized in Section 5.

2 GAMMA-GAMMA ABSORPTION

$\gamma - \gamma$ absorption imposes a restriction on the maximum energy of the γ -rays emitted by a compact source (Guilbert et al. 1983). This provides a test for whether the observed γ -rays can be emitted by an accretion disc or if they should be associated with a relativistic jet or a more complicated geometry of the source (Illarionov & Krolik 1996). Such a test has been applied to γ -loud AGNs (e.g., McNaron-Brown et al. 1995; Becker & Kafatos 1995).

2.1 The model

Consider a homogeneous γ -ray emitting disc of radius R and assume that the hard X/ γ -ray emission emerging from the disc is isotropic and has a power-law spectrum around 511 keV with intensity (flux per unit energy per steradian)

$$I_\varepsilon = I_1 \varepsilon^{-\alpha}, \quad (1)$$

where $\varepsilon = h\nu/m_ec^2$ is photon energy in units of the electron rest mass energy. The disc spectral luminosity is given by

$$L_\varepsilon = L_1 \varepsilon^{-\alpha}, \quad L_1 = 2\pi^2 R^2 I_1.$$

The main parameter of the model is the compactness parameter,

$$l_1 = \frac{L_1 \sigma_T}{m_e c^3 R}, \quad (2)$$

which can also be expressed in terms of the Eddington luminosity, $L_E = 2\pi r_g m_p c^3 / \sigma_T$,

$$l_1 = 2\pi \frac{m_p}{m_e} \frac{L_1}{L_E} \frac{r_g}{R},$$

where $r_g = 2GM/c^2$ is the gravitational radius of a black hole of mass M . We assume the typical spectral index $\alpha > 1$, then the γ -ray intensity steeply falls off towards high energies and l_1 roughly corresponds to the total luminosity above 511 keV. This luminosity is a few per cent of the bolometric luminosity of the disc in UV and X-rays.

2.2 Absorption inside and outside the source

For a rough estimate of $\gamma - \gamma$ absorption inside the source, take the $\gamma - \gamma$ opacity of an isotropic radiation field (Gould & Schréder 1967)

$$\kappa_{\gamma\gamma}^{\text{isotropic}}(\varepsilon) = \eta \sigma_T \frac{w(\varepsilon^{-1})}{m_e c^2} = \frac{2\eta l_1}{\pi R} \varepsilon^\alpha, \quad (3)$$

where $w(\varepsilon) = 4\pi I_\varepsilon / c$ is the spectral energy density of the radiation, and $\eta(\alpha)$ is a numerical factor, e.g., $\eta \approx 0.122, 0.072, 0.047$ for $\alpha=1, 1.5, 2$ respectively. The position of the spectral break due to absorption inside the source, ε_{\max} , can be estimated from the condition $\kappa_{\gamma\gamma}^{\text{isotropic}} h \sim 1$, where h is the disc thickness. Then one gets

$$\varepsilon_{\max} \sim \left(\frac{\pi}{2\eta l_1} \frac{R}{h} \right)^{1/\alpha}. \quad (4)$$

In the case $h \ll R$ this is a much weaker constraint than that for a spherical source with $h \sim R$. However, equation (4) is not the final answer to the problem of $\gamma - \gamma$ absorption because those γ -rays which have not been absorbed inside the disc-like source may be absorbed above the disc when passing through its radiation field (see also Zdziarski 1984).

Let us evaluate absorption for a γ -photon of energy ε emitted along the disc axis (z -axis) assuming for simplicity that the disc compactness is small ($l_1 < 1$) and the non-linear effects are unimportant. Then at height z the $\gamma - \gamma$ opacity seen by our photon is caused by the radiation propagating freely from the disc within an angle $\theta_{\max} = \arctan(R/z)$. Photons of energy ε' streaming at angle $\theta < \theta_{\max}$ can interact with our photon if ε' exceeds the threshold

$$\varepsilon_{\text{thr}} = \frac{2}{\varepsilon(1 - \cos \theta)}. \quad (5)$$

The $\gamma - \gamma$ opacity is then given by

$$\kappa_{\gamma\gamma}(\varepsilon, z) = \frac{l_1}{\pi \sigma_T R} \int_0^{\theta_{\max}} d\theta \sin \theta \int_{\varepsilon_{\text{thr}}(\theta, \varepsilon)}^{\varepsilon_{\max}} d\varepsilon' \varepsilon'^{-\alpha-1} \times (1 - \cos \theta) \sigma_{\gamma\gamma}(\varepsilon, \varepsilon', \theta), \quad (6)$$

where $\sigma_{\gamma\gamma}$ is the cross section for $\gamma - \gamma$ pair production (Jauch & Rohrlich 1976)

$$\sigma_{\gamma\gamma}(\varepsilon_c) = \frac{3\sigma_T}{8\varepsilon_c^2} \left[\left(2 + \frac{2}{\varepsilon_c^2} - \frac{1}{\varepsilon_c^4} \right) \ln \left(\varepsilon_c + \sqrt{\varepsilon_c^2 - 1} \right) - \left(1 + \frac{1}{\varepsilon_c^2} \right) \sqrt{1 - \frac{1}{\varepsilon_c^2}} \right], \quad (7)$$

$\varepsilon_c = (\varepsilon'/\varepsilon_{\text{thr}})^{1/2}$ is the energy of the interacting photons in the center-of-momentum frame. After integration we find

$$\kappa_{\gamma\gamma} = \frac{\eta l_1}{\pi R} 2^{-\alpha-1} (1 - \cos \theta_{\max})^{\alpha+2} \varepsilon^\alpha, \quad (8)$$

where

$$\eta(\alpha) = \frac{4}{\alpha+2} \int_1^\infty \varepsilon_c^{-2\alpha-1} \frac{\sigma_{\gamma\gamma}(\varepsilon_c)}{\sigma_T} d\varepsilon_c$$

is the numerical factor already appearing in equation (3) and calculated analytically in Svensson (1987). Since the integral peaks at $\varepsilon_c \sim 1$, the exact value of ε_{\max} is not important and we set $\varepsilon_{\max} = \infty$. Now from equations (3) and (8) we get

$$\frac{\kappa_{\gamma\gamma}}{\kappa_{\gamma\gamma}^{\text{isotropic}}} = \sin^{2\alpha+4} \left(\frac{\theta_{\max}}{2} \right) = \frac{1}{2^{\alpha+2}} \left(1 - \frac{z}{\sqrt{z^2 + R^2}} \right)^{\alpha+2}.$$

This function is shown in Fig. 1 for $\alpha = 1, 1.5, 2$. The opacity above the disc is strongly reduced because our photon moving along the disc axis does not encounter any radiation in the opposite direction which would dominate the $\gamma - \gamma$ opacity in the isotropic case.

It is interesting to compare the total optical depth seen by a γ -photon emitted along the disc axis, $\tau_{\gamma\gamma} = \int_0^\infty \kappa_{\gamma\gamma} dz$, with

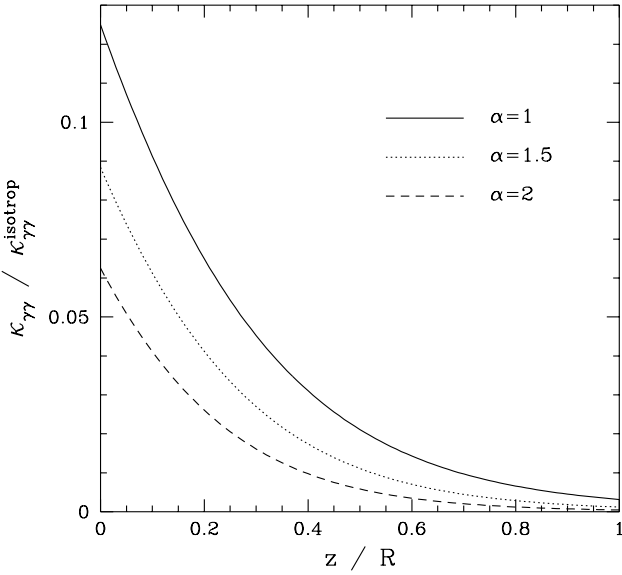


Figure 1. The ratio of $\gamma - \gamma$ opacity at height z above the disc to $\kappa_{\gamma\gamma}^{\text{isotropic}}$ given by equation (3). The opacity is calculated for γ -rays propagating along the disc axis. R is the disc radius, α is the spectral index of the radiation.

$R\kappa_{\gamma\gamma}^{\text{isotropic}}$ which can be (very roughly) associated with the $\gamma - \gamma$ optical depth of a spherical source of the same intensity, I_ε , and dimension, R . We get

$$\frac{\tau_{\gamma\gamma}}{R\kappa_{\gamma\gamma}^{\text{isotropic}}} = \int_0^{\pi/2} \frac{\sin^{2\alpha+4}(\theta/2)}{\sin^2 \theta} d\theta.$$

The dependence of this ratio on α is shown in Fig. 2. E.g., for $\alpha = 1$, $\tau_{\gamma\gamma}$ is ≈ 30 times smaller than $R\kappa_{\gamma\gamma}^{\text{isotropic}}$. This result combined with equation (4) shows that the absorption constraint on γ -ray spectra is very sensitive to the source geometry and it can be much weaker than the usually used estimate for the spherical case.

2.3 Dependence on inclination angle

We now calculate the non-linear γ -ray transfer above the disc and study the dependence of the observed absorption break on the disc inclination to the line of sight. The bulk of $\gamma - \gamma$ reactions occur close to the disc surface (see Fig. 1), and we solve a simplified transfer problem in a one-dimensional approximation. In this approximation, the radiation field is taken to be axisymmetric and uniform on any slice $z = \text{constant}$, and the effect of the finite size of the disc is treated for an optically thin atmosphere by truncating the radiation at angles $\theta > \theta_{\max}(z)$. We divide the slab $z < R/2$ above the disc into 25 horizontal layers, and assume that the radiation escapes freely from the last (upper) layer. The intrinsic boundary condition is the isotropic power-law radiation given by equation (1). To get a stationary solution, $I_\varepsilon(z, \theta)$, we take an initially empty atmosphere and let the γ -rays propagate from the disc. We then follow the evolution of the radiation field in the computational slab until a stationary state is established. Further details of the numerical method are given in Appendix A.

Examples of spectra emerging at different angles from the disc with a modest compactness $l_1 = 25$ and spectral index $\alpha = 1.5$ are

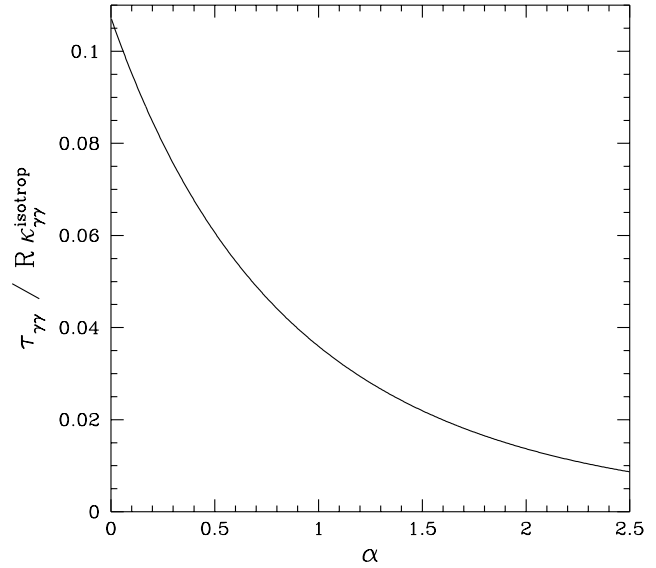


Figure 2. The ratio of the $\gamma - \gamma$ optical depth seen by a gamma photon emitted along the disc axis to $R\kappa_{\gamma\gamma}^{\text{isotropic}}$; α is the spectral index of the radiation.

shown in Fig. 3. We included only the $\gamma - \gamma$ reaction in the transfer problem in order to see the efficiency of pure absorption. The other two non-linear effects, Compton scattering and annihilation emission of the produced pairs, become important when $l_1 \gtrsim 30$ as the atmosphere becomes optically thick, see Section 3.1.

A qualitative dependence on the inclination angle θ is seen in Fig. 3: Absorption is more efficient at large inclinations. At large θ , an emitted γ -photon travels a long path at small heights where the $\gamma - \gamma$ opacity is large. Such a photon encounters especially high opacity because the threshold condition (5) is weaker at large θ . As a result, the escape probability is strongly reduced.

3 OPTICALLY THIN PAIR WIND

Each $\gamma - \gamma$ interaction produces one e^\pm pair. Therefore, the solution to the transfer problem in Section 2.3 automatically gives the pair injection rate, $\dot{n}_+^{\gamma\gamma}$, as a function of the height z above the disc. The bulk of pairs are injected close to the disc surface and are immediately cooled by the soft radiation down to the Compton temperature of the radiation field, $kT_C \sim 1 - 10$ keV. The time-scale for Compton cooling is given by

$$t_C = \frac{3m_e c}{8\sigma_{\text{Tw}}} = \frac{3}{16} \frac{m_e}{m_p} \frac{R}{c} \left(\frac{L}{L_E} \right)^{-1} \left(\frac{R}{r_g} \right), \quad (9)$$

where $w = L/\pi R^2 c$ is the radiation energy density, L is the disc luminosity. Here only luminous discs are considered, and t_C is shorter than the time-scale for pair escape, $t_{\text{esc}} \sim R/c$. On the time-scale t_C , pairs are also accelerated by the pressure of soft radiation. The e^\pm plasma is light and the gravitational force can be neglected as compared to the radiative force when $L > (m_e/m_p)L_E$. Then pairs acquire an equilibrium bulk velocity for which the radiation pressure is balanced by the radiation drag. Near the disc surface, where the radiation field is semi-isotropic, the equilibrium velocity is about $0.45c$ (Icke 1989; see also Section 4.2).

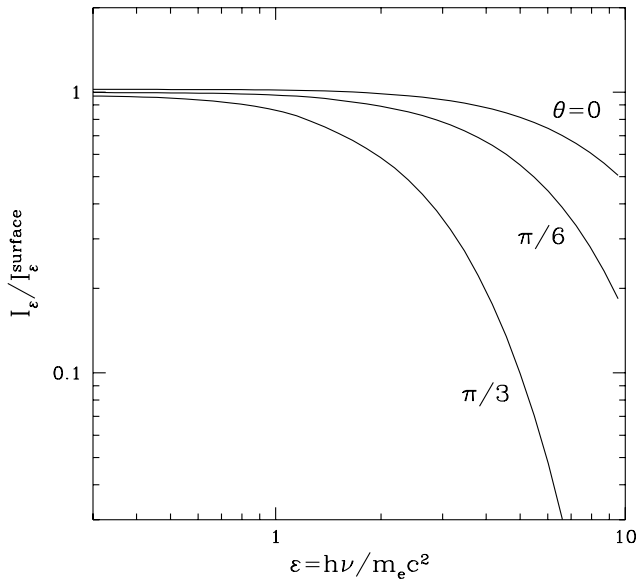


Figure 3. The $\gamma - \gamma$ absorption observed at inclination angles $\theta = 0, \pi/6, \pi/3$ from a disc with compactness $l_1 = 25$ and spectral index $\alpha = 1.5$. I_e^{surface} is the radiation intensity at the disc surface given by equation (1). I_e is the intensity of the emerging radiation found by numerical simulation of the γ -ray transfer above the disc. Compton scattering and annihilation emission in the e^\pm atmosphere are neglected.

Table 1. The efficiency of γ -ray transformation into an e^\pm -wind

l_1	5	10	15	20	25	30
L_\pm/L_1	0.04	0.07	0.09	0.10	0.11	0.12

3.1 Luminosity in pair rest mass

In an optically thin wind, pairs escape before they can annihilate since t_{esc} is less than the time-scale for annihilation, $t_{\text{ann}} \sim (n_+ \sigma_{\text{T}} c)^{-1}$. Then the flux of escaping pairs equals the column rate of pair production above the disc. The corresponding flux of e^\pm rest-mass energy equals

$$F_\pm = 2m_e c^2 \int_0^{R/2} \dot{n}_+^{\gamma\gamma}(z) dz.$$

The total rest-mass energy carried away by the e^\pm wind can be estimated as

$$L_\pm = 2\pi R^2 F_\pm.$$

In the limit of small compactness, γ -rays propagate almost freely in the atmosphere, and only a small fraction of L_1 is transformed into L_\pm . This fraction is proportional to the $\gamma - \gamma$ optical depth which, in turn, is proportional to l_1 . Therefore, in the limit of small compactness $L_\pm/L_1 \propto l_1$. As l_1 increases, $\gamma - \gamma$ absorption significantly depletes MeV photons, which reduces the $\gamma - \gamma$ opacity. The transfer becomes non-linear and L_\pm/L_1 saturates at $\lesssim 20\%$. Numerically calculated values of L_\pm/L_1 for several compactnesses l_1 are given in Table 1. In the calculations, a spectral index $\alpha = 1.5$ was assumed.

Pairs escape with velocities $\sim c/2$, and the density of the at-

mosphere can be estimated as $n_+ \sim L_\pm/2\pi R^2 m_e c^3$. The typical scattering optical depth of the e^\pm -cloud around the disc is then given by

$$\tau_{\text{T}} \sim 2n_+ \sigma_{\text{T}} R \sim \frac{l_1}{\pi} \left(\frac{L_\pm}{L_1} \right). \quad (10)$$

Using Table 1, one can see that the atmosphere becomes optically thick when $l_1 \sim 30$.

In an optically thick wind, t_{ann} would become comparable to t_{esc} . Then L_\pm is limited by annihilation which depletes the particle population in the wind. The density of escaping pairs is controlled by the condition $t_{\text{ann}} \sim t_{\text{esc}}$ which gives $n_+ \sim (\sigma_{\text{T}} R)^{-1}$ and the upper limit for L_\pm (Phinney 1983; Guilbert & Stepney 1985; Ghisellini et al. 1992),

$$L_\pm^{\text{max}} \sim \frac{2\pi m_e c^3 R}{\sigma_{\text{T}}}, \quad (11)$$

which corresponds to compactness $l_\pm \sim 2\pi$.

3.2 Annihilation emission

Consider a plasma volume dV moving with velocity $\mathbf{v} = \beta c$. In the comoving frame, the number of annihilation photons emitted by this volume into solid angle $d\tilde{\Omega}$ during time $d\tilde{t}$ equals

$$dN = \frac{3}{16\pi} c \sigma_{\text{T}} \tilde{n}_+^2 d\tilde{V} d\tilde{t} d\tilde{\Omega},$$

where $\tilde{n}_+ = n_+/\gamma$ is the pair density in the comoving frame, $d\tilde{V} = \gamma dV$, and $\gamma = (1 - \beta^2)^{-1/2}$. In lab frame, these photons propagate within a solid angle $d\Omega = d\tilde{\Omega} \varepsilon_{\text{ann}}^{-2}$, where $\varepsilon_{\text{ann}} = \gamma^{-1}(1 - \beta \cdot \Omega)^{-1}$ is the photon energy in lab frame. Taking into account the invariance of four-volume, $d\tilde{V} d\tilde{t} = dV dt$, we get the annihilation power emitted in direction Ω by a unit volume of a stationary wind,

$$Q_{\text{ann}}(\Omega) = \frac{\varepsilon_{\text{ann}} m_e c^2 dN}{dV dt d\Omega} = \frac{3m_e c^3 \sigma_{\text{T}} n_+^2}{16\pi \gamma^5 (1 - \beta \cdot \Omega)^3}.$$

Note that the fraction of photons emitted within a solid angle $d\Omega$ equals $d\Omega \varepsilon_{\text{ann}}^2/4\pi$. The average energy of the annihilation photons equals $\gamma m_e c^2$.

A mildly relativistic bulk motion makes the wind emission considerably different from that of a cold source at rest:

i) Q_{ann} is significantly anisotropic even for a modest β . E.g., for $\beta = 0.5$ the emission in the flow direction is 8 times larger than in the perpendicular direction.

ii) The annihilation photons are blueshifted in the lab frame by a factor of $[\gamma(1 - \beta \cdot \Omega)]^{-1}$. For a face-on-oriented observer and $\beta = 0.5$ the blueshift equals $\sqrt{3}$.

iii) The width of the annihilation line is determined by the velocity gradients in the wind rather than by the thermal motions. The bulk velocities are relativistic, so the line must be broad.

The total power of the annihilation emission can be roughly estimated as

$$L_{\text{ann}} \sim \left(\frac{t_{\text{esc}}}{t_{\text{ann}}} \right) L_\pm \sim \tau_{\text{T}} L_\pm,$$

where τ_{T} is the typical scattering optical depth of the atmosphere, see equation (10). In the limit of small compactnesses, L_{ann}/L_1 falls off $\propto l_1^3$. Then annihilation of pairs produced inside the source is likely to dominate, and a narrow line at 511 keV might be expected. In the case of large compactnesses, where the atmosphere becomes optically thick, the line produced inside the source

must be scattered above the disc. The observed annihilation emission is then dominated by the e^\pm outflow which produces a broad blueshifted line as discussed in next Section.

4 OPTICALLY THICK OUTFLOW

We now address the formation of an optically thick outflow by calculating the γ -ray transfer above a disc with a compactness $l_1 > 30$. The main conversion of γ -rays into e^\pm pairs occurs close to the disc surface, at heights $z \ll R$ (see Section 4.1). We therefore consider a simplified one-dimensional transfer problem, in which pair production is calculated in a slab $0 < z < R/2$. We thus neglect the boundary effects connected with the finite size of the disc. The radiation is assumed to escape freely at the outer boundary $z = R/2$. Further calculations verify that this is a reasonable first approximation.

A magnetic field may affect the outflow dynamics if the magnetic pressure exceeds the radiation pressure. The configuration of the accretion disc magnetosphere is, however, quite uncertain. We assume here that the magnetic field does not prevent the vertical e^\pm outflow.

In an optically thick outflow $t_{\text{ann}}/t_{\text{esc}} \sim (n_+ \sigma_T R)^{-1} < 1$, i.e., pairs annihilate before they can escape. The bulk of e^\pm form a thermal population at the Compton temperature, $kT_C \sim 1 - 10$ keV, and only a small fraction form a non-thermal tail. The tail consists of those pairs which are braking after their creation towards thermal energies due to inverse Compton (IC) cooling by soft radiation and Coulomb collisions with the thermal e^\pm plasma. The stationary energy distribution of the braking particles peaks at semi-relativistic energies (Beloborodov & Illarionov 1995). The density of non-thermal pairs $n_+^{\text{nth}} \approx \dot{n}_+^{\gamma\gamma} t_C$ is a small fraction, $\sim t_C/t_{\text{ann}}$, of the thermal population, n_+ .

The pairs are created in the interactions between MeV photons and they typically have initial Lorentz factors $\gamma \sim 2 - 3$. IC photons produced in the slab therefore have modest energies $\varepsilon_{\text{IC}} \sim \gamma^2 \varepsilon_s \lesssim 50$ keV, where ε_s is the energy of a soft photon before upscattering, typically in the range 1 eV – 10 keV. (The non-thermal component is optically thin and repeated upscatterings are negligible.) It means that the kinetic energy of created pairs is just absorbed by the soft component of radiation and a negligibly small fraction is converted into hard radiation. We therefore neglect the presence of non-thermal pairs in the calculations of hard X/ γ -ray transfer and assume that the plasma is composed of the cold thermal pairs only. Then there are only two sources of hard photons: the primary source below the computational slab and the annihilation emission of pairs produced in the slab.

In calculations of Compton scattering by thermal e^\pm we neglect their slow thermal motions and account for the fast bulk motion which strongly affects the scattering process. The plasma has a bulk velocity near the equilibrium value $v \sim 0.5c$ determined by the soft radiation which dominates the energy density of the atmosphere. The equilibrium velocity can be found as a function of optical depth independently of the atmosphere density profile (see Section 4.2). The velocity varies from $0.3c$ to $0.7c$. As a first step, we adopt $\beta = v/c = 0.5$ in the simulations of the γ -ray transfer.

4.1 Numerical model of outflow formation

We have calculated several transfer models assuming an isotropic source (1) below the computational slab. Details of the code are given in Appendix A.

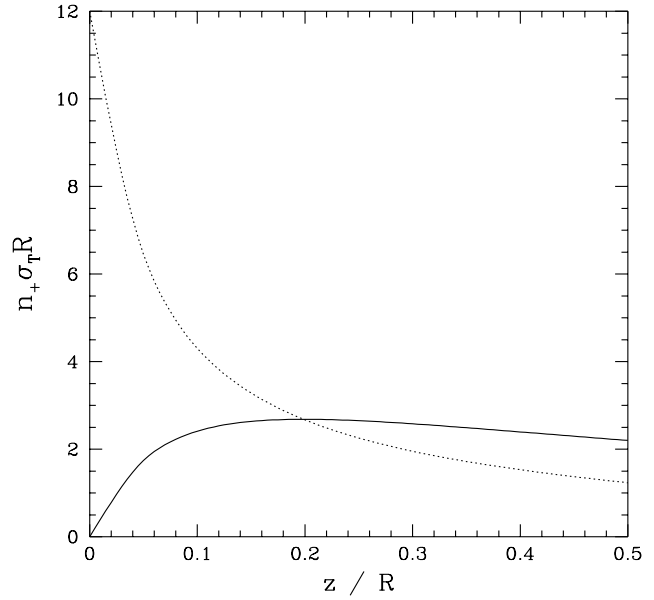


Figure 4. The density profile of the e^\pm outflow created above a disc with compactness $l_1 = 150$ and spectral index $\alpha = 1.5$ (solid curve). The dotted curve shows the density n_+^* which would correspond to the local balance between pair production and annihilation.

We here consider the case where there is no e^\pm flux from the γ -ray source and set $n_+ = 0$ at $z = 0$. Then the outflow is created above the source. An example of the density profile obtained for the atmosphere above a disc with a compactness $l_1 = 150$ and a spectral index $\alpha = 1.5$ is shown in Fig. 4. The equilibrium density, $n_+^*(z)$, would correspond to local balance between pair production and annihilation, i.e., $\dot{n}_+^{\gamma\gamma} = (3/8)(1 - \beta^2)\sigma_T c n_+^{*2}$. The pair density, n_+ , strongly deviates from n_+^* as a result of pair advection along the z -axis. The e^\pm transfer equation in the stationary case can be written as

$$\beta \frac{dn_+}{dz} = \frac{3}{8}(1 - \beta^2)\sigma_T [n_+^{*2} - n_+^2].$$

The first and second terms in the square brackets stand for e^\pm production and annihilation respectively. At large heights, advection results in that $n_+ > n_+^*$ and pair production becomes unimportant: the outflow is dominated by pairs advected from the lower layers. The evolution of the pair density with height is then governed mainly by annihilation.

The steep decrease in n_+^* shows that the rate of pair injection, $\dot{n}_+^{\gamma\gamma} \propto n_+^{*2}$, steeply decreases with height as a result of strong degradation of the γ -rays*. Roughly, the outflow is created in the “injection zone”, $z/R \lesssim 0.2$, where $n_+ < n_+^*$. The created pair plasma then outflows in the “annihilation zone”, $z \gtrsim 0.2$, where $n_+ > n_+^*$.

The intensity of the outgoing γ -rays is suppressed to such an extent that the equilibrium pair density becomes $n_+^* \sim (\sigma_T R)^{-1}$ which is also the typical density of the “false photosphere”. At $z \sim$

* Note that the radiation quickly becomes anisotropic in the low layers because of preferential depletion of γ -rays at large θ . The boundary effects are therefore reduced and the slab geometry may be a good approximation, in contrast to the optically thin case where the finiteness of the disc radius was important and we truncated the radiation at $\theta > \arctan(R/z)$.

R we get $n_+ \sim (\sigma_T R)^{-1}$, i.e., we are already in the transition zone between the optically thick e^\pm envelope and an optically thin wind from the envelope. At $z > R$ the flow is no longer plane-parallel and the pair density is strongly reduced. Our code is not able to follow the transition to the optically thin wind. One can only estimate the flux of escaping pairs as $\sim c/\sigma_T R$. The emerging luminosity in e^\pm rest mass is given by equation (11).

We now briefly discuss the annihilation emission of the outflow shown in Fig. 4. Only photons emitted perpendicular to the disc have a significant chance (~ 0.5) to escape the optically thick layers, and the bulk of photons emitted at large angles will be down-scattered or absorbed. The escaping photons will be detected by a distant observer as an annihilation line. In the numerical simulation we obtained a line in the emerging spectrum located at $\varepsilon_{\text{ann}} = [\gamma(1 - \beta \cos \theta)]^{-1}$ where $\beta = 0.5$ is the atmospheric velocity and θ is inclination angle. With increasing inclination, the line flux as well as the continuum γ -ray emission decreases by 10 – 30 times. The equivalent width of the line is $\sim \varepsilon_{\text{ann}}/2$ at all inclinations. A model taking into account the velocity gradient in the optically thick layers (see Section 4.2) would yield a broad annihilation bump of approximately the same equivalent width.

4.2 Collimation of soft radiation

The γ -ray flux converted into pairs above the disc is much smaller than the flux of soft radiation. The latter, being approximately equal to the total energy flux from the disc, is constant in the optically thick e^\pm outflow. However, scattering in the outflow changes the angular distribution of the soft radiation.

The scattering mainly occurs in the optically thick layers, $z < R$, where the outflow is approximately plane-parallel. We consider the simplified one-dimensional problem of radiative transfer in a slab of vertically outflowing pair plasma atop an isotropic source of soft radiation. Each electron/positron moves in Compton equilibrium during its life-time in the e^\pm envelope. The equilibrium velocity at each height is determined by the local angular distribution of the frequency-integrated intensity of the radiation, I .

In the plane-parallel geometry, the intensity is a function of the angle θ between the ray and the z -axis, and of the optical depth in the e^\pm envelope, $d\tau = -2n_+ \sigma_T dz$. The only parameter of the problem is the column density of the envelope, τ_0/σ_T . Here we neglect the polarization of radiation due to scattering (polarization is considered in Beloborodov 1998). The transfer equation then reads

$$\frac{1}{2n_+ \sigma_T c} \frac{\partial I}{\partial t} - \cos \theta \frac{\partial I}{\partial \tau} = (1 - \beta \cos \theta)(S - I), \quad 0 < \tau < \tau_0, \quad (12)$$

The radiation scattered in direction Ω is represented by the source function,

$$S(\Omega) = \frac{1}{\sigma_T (1 - \beta \cdot \Omega)} \int I(\mathbf{n}) \frac{d\sigma}{d\Omega}(\mathbf{n}) \frac{\varepsilon'}{\varepsilon} d\mathbf{n}, \quad (13)$$

where \mathbf{n} is the direction of a photon before scattering and $d\sigma/d\Omega$ is the differential cross section for Thomson scattering. ε and ε' are the photon energies before and after the scattering respectively, and they are related by the equation

$$\varepsilon'(1 - \beta \cdot \Omega) = \varepsilon(1 - \beta \cdot \mathbf{n}), \quad (14)$$

which expresses the fact that the photon energy does not change in the comoving frame.

The equilibrium velocity β is determined at each height by the equation

$$(1 + \beta^2)I_1 - \beta(I_0 + I_2) = 0, \quad (15)$$

where

$$I_m = \frac{1}{4\pi} \int I(\theta) \cos^m \theta d\Omega.$$

The equilibrium equation expresses the condition that the net flux of radiation in the comoving frame vanishes (see, e.g., Sikora & Wilson 1981), and in the lab frame it means that the radiation pressure is balanced by the radiation drag. Pairs keep their velocity near the equilibrium value which varies with height. The time-scale for relaxation to the equilibrium $\sim t_C$ is the shortest time-scale in the problem, therefore, the equilibrium velocity is a strong attractor in phase space, and we neglect deviations of β from that given by equation (15). The equations (12) and (15) then form a closed set of equations.

We are looking for a stationary solution, $\partial I/\partial t = 0$. The first and second moments of the radiation field are integrals of the problem, $I_1(\tau) = \text{constant}$ and $I_2(\tau) = \text{constant}$, (in contrast to the classical problem of radiative transfer in an electron medium at rest, which has only $I_1(\tau) = \text{constant}$). The constancy of I_2 can easily be checked by combining the first moment of equation (12) with the condition (15). $I_2(\tau) = \text{constant}$ is just another way to express the equilibrium condition: $4\pi I_2/c$ equals the radiation pressure in the vertical direction, and its gradient vanishes in the equilibrium e^\pm envelope.

Another special feature of the equilibrium radiative transfer is that the radiation density inside an e^\pm envelope cannot be strongly enhanced regardless the optical depth of the envelope. The trapped radiation is advected out of the optically thick layers with a velocity $\sim c/2$, and the presence of the envelope around the disc weakly affects the radiation density, as can also be derived formally using $I_2(\tau) = \text{constant}$. The main impact of e^\pm is on the angular distribution of radiation.

Here we adopt a simplified model for Thomson scattering. We will assume that the scattered radiation is isotropic in the comoving frame, i.e., a fraction $d\tilde{\Omega}/4\pi$ of the scattered photons have directions within the solid angle $d\tilde{\Omega}$. The solid angle corresponding to $d\tilde{\Omega}$ in lab frame equals $d\Omega = \gamma^2(1 - \beta \cdot \Omega)^2 d\tilde{\Omega}$ (see, e.g., Rybicki & Lightman 1979). The total scattering cross section equals $\sigma = \sigma_T(1 - \beta \cdot \mathbf{n})$, and the differential cross section for the scattering in the lab frame is given by

$$\frac{d\sigma}{d\Omega} = \frac{\sigma_T}{4\pi} \frac{1 - \beta \cdot \mathbf{n}}{\gamma^2(1 - \beta \cdot \Omega)^2}.$$

Equations (13) and (14) then give the source function

$$S(\theta) = \frac{I_0 - 2\beta I_1 + \beta^2 I_2}{\gamma^2(1 - \beta \cos \theta)^4}.$$

Using the equilibrium condition (15), we express I_2 in terms of I_0 , I_1 , and β , and rewrite $S(\theta)$ as

$$S(\theta) = \frac{I_0 - \beta I_1}{\gamma^4(1 - \beta \cos \theta)^4}. \quad (16)$$

We solve the equations (12) and (15) with the source function (16) numerically. At the inner boundary ($\tau = \tau_0$), we set a source of isotropic soft radiation, which absorbs photons impinging back on the disc (the results are essentially the same if we assume reflection at the inner boundary). At the outer boundary ($\tau = 0$), we assume free escape of the radiation. As initial conditions we assume that a semi-isotropic radiation is filling the atmosphere at all heights (curve 1 in Fig. 5b). This would be a stationary solution if the atmosphere were optically thin (the corresponding equilib-

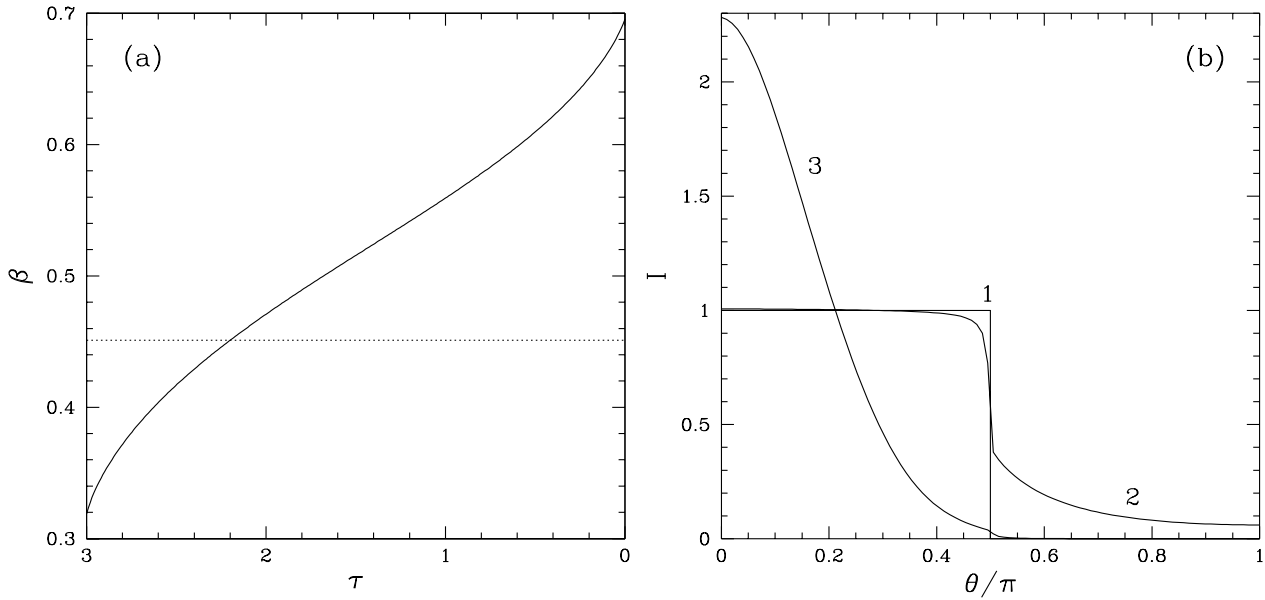


Figure 5. The stationary solution for the soft radiation transfer in a plane-parallel e^\pm atmosphere with column density $3\sigma_T^{-1}$: (a) Velocity profile. Parameter τ is defined as $d\tau = -2n_+\sigma_T dz$. The dotted line displays the equilibrium velocity in a semi-isotropic radiation field. (b) The angular dependence of the soft radiation intensity: 1 – as emitted by the disc, 2 – at the base of the atmosphere ($\tau = 3$), 3 – as emerging from the atmosphere ($\tau = 0$). The intensity is normalized so that $I(\Omega) = 1$ for the radiation emitted by the disc.

rium velocity $c(4 - \sqrt{7})/3 \approx 0.45c$ is shown by the dotted line in Fig. 5a). The initial state evolves due to Thomson scattering in the atmosphere. The stationary solution $I(\tau, \theta), \beta(\tau)$ that we are looking for depends only on the parameter τ_0 and does not depend on the density profile, $n_+(z)$. We therefore choose the simplest density profile, $n_+(z) = \text{constant}$. In the calculations, we use a grid which is homogeneous in the z - and θ -direction. The number of grid points is $N_z \times N_\theta = 300 \times 100$. The chosen time step equals $\Delta t = 0.3\tau_0/2n_+\sigma_T c N_z$.

The resulting stationary solution for $\tau_0 = 3$ is presented in Fig. 5a,b. In the lowest layers of the slab, the equilibrium velocity is less than $0.45c$ since, besides the semi-isotropic disc radiation, there is some flux in the opposite direction as a result of the radiation being backscattered by the outflow (see Fig. 5b, curve 2). In higher layers, the radiation gets collimated by scattering on the moving pairs, and the equilibrium velocity increases to $\sim 0.7c$. The angular distribution of the outgoing radiation is shown by curve 3 in Fig. 5b. The distribution does not depend on τ_0 in the optically thick limit, and therefore does not depend on the compactness of the primary γ -ray source. The emerging radiation is significantly anisotropic, e.g., the intensity at $\theta = \pi/3$ is ~ 7 times smaller than that at $\theta = 0$.

4.3 Acceleration of escaping pairs

The escaping pairs form an optically thin wind. At large heights, $z \gg R$, the angular size of the central luminous disc $R \sim r_g$ diminishes and the escaping pairs are accelerated. Their equilibrium Lorentz factor is determined by the balance between pressure of the central radiation and drag by the radiation from the outer parts of the disc (Phinney 1987). With increasing height the density of the central radiation is reduced $\propto z^{-2}$ and redshifted in the co-moving frame as γ^{-2} . The density of the diffuse radiation from

the outer parts of the disc scales $\propto z^{-3}$, but it is blueshifted as γ^2 . The resulting equilibrium Lorentz factor $\gamma_{\text{eq}} \sim (z/r_g)^{1/4}$. At large distances from the black hole, the pair Lorentz factor falls below the equilibrium value because of radiation dilution, and saturates at $\gamma_\infty \sim (m_p L / m_e L_E)^{1/7}$, where L is the disc luminosity, L_E is the Eddington limit.

The collimation of the central radiation may increase γ_∞ . The relevant collimation parameter, ζ , equals the ratio of the collimated intensity at $\theta = 0$ to the intensity of isotropic radiation of the same net flux. In our case $\zeta \approx 2.3$, see Fig. 5b. Accounting for the collimation, the equilibrium Lorentz factor can be estimated as $\gamma_{\text{eq}} \sim \zeta^{1/4} (z/r_g)^{1/4}$. At some height z_* , γ falls below γ_{eq} . At heights $z \gg z_*$, the drag is negligible and the acceleration is determined by the central radiation flux $F = \zeta L / 4\pi z^2$,

$$\dot{\gamma} \approx \frac{\sigma_T F}{4\gamma^2 m_e c^2}.$$

Substituting $\dot{\gamma} \approx c(d\gamma/dz)$ and integrating this equation gives the asymptotic solution

$$\gamma^3(z) = \gamma_\infty^3 - \frac{3}{8} \frac{m_p}{m_e} \frac{\zeta L}{L_E} \frac{r_g}{z}, \quad z \gg z_*.$$

The falling of γ below γ_{eq} and transition to the regime $\gamma \ll \gamma_{\text{eq}}$ occurs when the acceleration time-scale, $\gamma/\dot{\gamma}$, equals the escape time-scale, z/c . At $z = z_*$ one therefore has the condition $8\gamma^3(z/r_g) \approx (m_p/m_e)(\zeta L/L_E)$. By matching the solutions for the two regimes $\gamma = \gamma_{\text{eq}}$ and $\gamma \ll \gamma_{\text{eq}}$ at $z = z_*$, one can estimate z_* and then γ_∞ ,

$$\gamma_\infty \approx \zeta^{2/7} \left(\frac{m_p}{m_e} \frac{L}{L_E} \right)^{1/7}. \quad (17)$$

The weak dependence on ζ shows that γ_∞ is not crucially affected by the collimation of the central radiation. To obtain large Lorentz factors $\sim 10 - 20$ observed in AGN jets, a collimation factor $\zeta \sim 10^2$ would be required.

5 CONCLUSIONS

MeV photons are strongly absorbed above a compact disk-like source and the observed γ -ray luminosity is suppressed, especially if the disc is viewed at large inclinations. The pair plasma created above the disc flows away in Compton equilibrium with the soft radiation field. The optical depth of the outflow depends on the γ -ray compactness, l_1 , (see Section 2.1 for the definition of l_1). The outflow is optically thin if $l_1 < 30$ and becomes optically thick if $l_1 \gtrsim 30$. In the optically thin case, pairs escape without annihilation and the emerging luminosity in pair rest mass corresponds to the number of γ -photons absorbed above the disc.

The optically thick outflow can be described as an envelope surrounding the disc where the created pairs have a life-time less than the escape time-scale. During their life-time pairs move in equilibrium with the soft radiation field with a velocity $\sim 0.5c$. Detailed calculations of the optically thick outflow show that its velocity increases from $\approx 0.3c$ at the base to $\approx 0.7c$ at the photosphere. In the photospheric layers, $z \sim R$, the pair density reduces to $n_+ \sim (\sigma_T R)^{-1}$, R being the radius of the γ -ray emitting disc. A significant fraction of pairs created in these layers escape to produce a luminosity in pair rest mass $L_\pm \sim 2\pi m_e c^3 R / \sigma_T$.

The condition for formation of an optically thick e^\pm outflow is likely to be fulfilled in the brightest objects, such as quasars, especially if the black hole has a large spin. The bulk of the energy is then released in a very compact region, $R \approx r_g$, and the outflow becomes optically thick if the luminosity above 511 keV exceeds a small fraction, $\sim 3 \times 10^{-3}$, of the Eddington luminosity. The optically thick outflow will strongly affect the observed radiation:

i) The luminosity of the central region becomes anisotropic as a result of scattering in the outflow. The apparent bolometric luminosity of the disc is then suppressed if the disc is viewed at large inclinations.

ii) The outflow obscures the central region of the accretion disc and inhibits observation of reflection features, in particular the Fe K α line. Reflected X-rays may be observed from the outer parts of the disc which is illuminated by the central source. However, because of the strong anisotropy of the source, the reflection features should be weak. This may explain the lack of Fe K α lines in bright radio-quiet quasars compared with lower luminosity Seyfert AGNs (Reeves et al. 1997).

iii) The expected annihilation line is blueshifted and broad due to the velocity gradient in the outflow. The line increases the continuum γ -ray flux by a factor of ~ 2 at 0.5 – 1 MeV, in contrast to the narrow annihilation feature at 511 keV usually expected from luminous γ -ray sources.

Even an outflow of a modest optical depth, ~ 0.1 , may affect the observed radiation by changing its polarization (Beloborodov 1998): the polarization vector becomes parallel to the disc axis, in agreement with optical observations of non-blazar AGNs (Antonucci 1992).

Our calculations of the pair production around the accretion disc are limited to the one-dimensional slab approximation. Simulations of the outflow formation in cylindrical geometry may provide new insights into compact γ -ray sources. The γ -ray emitting region of the disc has a finite radius and at large inclinations the slab approximation is not adequate as the bulk of observed hard radiation then comes from the boundary of the γ -ray emitting region. Simulations in cylindrical geometry would also allow the study of the interesting case where a source of GeV radiation is geometrically separated from the source of soft X-rays, being located in the centre of the surrounding X-ray ring (Illarionov & Krolik 1996). In

such a geometry, the e^\pm outflow would be created in a cylindrical wall between the two sources.

ACKNOWLEDGMENTS

I am grateful to the referee, P. Coppi, for useful comments, to R. Svensson, I. V. Igumenshchev, P. B. Ivanov, and especially to A. F. Illarionov for discussions. This work was supported by RFFI grant 97-02-16975 and the Swedish Natural Science Research Council. I thank M. Abramowicz and the Department of Astronomy & Astrophysics of Chalmers University of Technology, where a part of this work was done, for hospitality.

REFERENCES

Antonucci R. R. J., 1992, in Holt S., Neff S., Urry C.M., eds, AIP Conf. Proc. 254, Testing the AGN Paradigm. New York, p. 486
 Becker P. A., Kafatos M., 1995, ApJ, 453, 83
 Beloborodov A. M., Illarionov A. F., 1995, ApJ, 450, 64
 Beloborodov A.M., 1998, ApJ, 496, L105
 Coppi P.S., Lamb D. Q., 1992, in Paciesas W. S., Fishman G. J., eds, AIP Conf. Proc. 265, Gamma-Ray Bursts. New York, p. 257
 Galeev A. A., Rosner R., Vaiana G. S., 1979, ApJ, 229, 318
 Ghisellini G., Celotti A., George I. M., Fabian A. C., 1992, MNRAS, 258, 776
 Gould R. J., Schréder G. P., 1967, Phys. Rev., 155, 1404
 Guilbert P. W., Fabian A. C., Rees M. J., 1983, MNRAS, 205, 593
 Guilbert P. W., Stepney S., 1985, MNRAS, 212, 523
 Gurevich L. E., Rumyantsev A. A., 1965, Sov. Physics – JETP, 20, 1233
 Herterich K., 1974, Nat, 250, 311
 Icke V., 1989, A&A, 216, 294
 Illarionov A. F., Krolik J. H., 1996, ApJ, 469, 698
 Jauch J. M., Rohrlich F., 1976, The Theory of Photons and Electrons. Springer, New York
 Katz J.I., 1982, ApJ, 260, 371
 Li H., Liang E.P., 1996, ApJ, 458, 514
 McNaron-Brown K. et al., 1995, ApJ, 451, 575
 Phinney S., 1983, PhD thesis, University of Cambridge
 Phinney S., 1987, in Zenus J. A., Pearson T. J., eds, Superluminal Radio Sources. Cambridge Univ. Press, p. 301
 Reeves J. N., Turner M. J. L., Ohashi T., Kli T., 1997, 292, 468
 Rybicki G.B., Lightman A.P., 1979, Radiative Processes in Astrophysics, Wiley, New York
 Sikora M., Wilson D. B., 1981, MNRAS, 197, 529
 Shapiro S. L., Lightman A. P., Eardley D. M., 1976, ApJ, 204, 187
 Svensson R., 1987, MNRAS, 227, 403
 Svensson R., 1996, A&AS, 120, 475
 Zdziarski A. A., 1984, A&A, 134, 301

APPENDIX A: NUMERICAL SIMULATION OF GAMMA-RAY TRANSFER

The radiation field in a plane-parallel atmosphere is axisymmetric at any height z . The photon distribution over energies, ε , and angles with respect to the z -axis, θ , is related to the radiation intensity by

$$n(\varepsilon, \theta) = \frac{2\pi \sin \theta I_\varepsilon}{\varepsilon m_e c^3}.$$

In the numerical simulations, we consider photon energies $0.1 < \varepsilon < 10$, and angles $0 < \theta < \pi$. The radiation field at each height is represented by photon numbers in $N_\varepsilon \times N_\theta = 50 \times 20$ cells which are logarithmically spaced in the ε -direction and uniformly spaced

in the θ -direction. We checked that our results are not significantly affected by doubling the grid resolution.

(i) $\gamma - \gamma$ reaction

To simulate the $\gamma - \gamma$ process we need the corresponding effective cross sections for the interaction between photons from cells $(i_\varepsilon, i_\theta)$ and $(i'_\varepsilon, i'_\theta)$. Given an angle between the interacting photons, ξ , and exact values of their energies, ε and ε' , one can calculate the $\gamma - \gamma$ cross section using equations (5) and (7) with θ replaced by ξ . To find the effective cross section for the interaction between two given cells we use the Monte-Carlo method. We calculate the cross section for randomly chosen values ε, θ and ε', θ' within the cells $(i_\varepsilon, i_\theta)$ and $(i'_\varepsilon, i'_\theta)$ and randomly chosen azimuthal angles of the interacting photons. We then find the average cross section for $\gamma - \gamma$ interaction between cells $(i_\varepsilon, i_\theta)$ and $(i'_\varepsilon, i'_\theta)$. Repeating this procedure for each pair of cells, we get a matrix Γ of size $N_\varepsilon \times N_\theta \times N_\varepsilon \times N_\theta$ containing the effective cross sections. The rate of photon depletion in each cell due to $\gamma - \gamma$ reaction is given by

$$\dot{n}_{\gamma\gamma}(i_\varepsilon, i_\theta) = c n(i_\varepsilon, i_\theta) \sum_{i'_\varepsilon, i'_\theta} \Gamma(i_\varepsilon, i_\theta, i'_\varepsilon, i'_\theta) n(i'_\varepsilon, i'_\theta).$$

(ii) Compton scattering

We also use the Monte-Carlo method to calculate the effective cross section for scattering from cell $(i_\varepsilon, i_\theta)$ to cell $(i'_\varepsilon, i'_\theta)$. In each Monte-Carlo event, we take a random photon energy ε and angle θ within the cell $(i_\varepsilon, i_\theta)$, and calculate the total scattering cross section $\sigma = (1 - \beta \cos \theta)\tilde{\sigma}$. Here β is the plasma velocity (in units of the speed of light) directed along the z -axis, and $\tilde{\sigma}$ is the total cross section in the comoving frame (Jauch & Rohrlich 1976)

$$\tilde{\sigma} = \frac{3\sigma_T}{8\tilde{\varepsilon}} \left[\frac{1}{2} + \frac{4}{\tilde{\varepsilon}} - \frac{1}{2(1+2\tilde{\varepsilon})^2} + \left(1 - \frac{2}{\tilde{\varepsilon}} - \frac{2}{\tilde{\varepsilon}^2}\right) \ln(1+2\tilde{\varepsilon}) \right],$$

where $\tilde{\varepsilon} = \gamma(1 - \beta \cos \theta)\varepsilon$ is photon energy in the comoving frame. The photon angle in the comoving frame is given by

$$\cos \tilde{\theta} = \frac{\cos \theta - \beta}{1 - \beta \cos \theta}.$$

Then we perform a random scattering in the comoving frame. The differential cross section for Compton scattering is given by (Jauch & Rohrlich 1976)

$$\frac{d\tilde{\sigma}}{d\tilde{\Omega}} = \frac{3\sigma_T}{16\pi} \frac{1}{[1 + \tilde{\varepsilon}(1 - \mu)]^2} \left[1 + \mu^2 + \frac{\tilde{\varepsilon}^2(1 - \mu)^2}{1 + \tilde{\varepsilon}(1 - \mu)} \right],$$

where $\mu = \tilde{\Omega} \cdot \tilde{\Omega}'$, $\tilde{\Omega}$ and $\tilde{\Omega}'$ being the photon directions before and after the scattering respectively. The photon energy after the scattering equals

$$\tilde{\varepsilon}' = \frac{\tilde{\varepsilon}}{1 + \tilde{\varepsilon}(1 - \mu)}.$$

Performing the inverse transformation to the lab frame, we get the energy, ε' , and angle, θ' , of the scattered photon, and determine the corresponding cell $(i'_\varepsilon, i'_\theta)$ into which it has been scattered. Repeating $1.5 \cdot 10^6$ Monte-Carlo events for each cell $(i_\varepsilon, i_\theta)$, we find the distribution of the scattered photons throughout all cells $(i'_\varepsilon, i'_\theta)$ and get a matrix $C(i_\varepsilon, i_\theta, i'_\varepsilon, i'_\theta)$ containing the required effective cross sections. The photon sink and source due to Compton scattering, \dot{n}_C^- and \dot{n}_C^+ respectively, are given by

$$\dot{n}_C^-(i_\varepsilon, i_\theta) = 2n_+ c n(i_\varepsilon, i_\theta) \tilde{\sigma}(i_\varepsilon, i_\theta),$$

$$\dot{n}_C^+(i_\varepsilon, i_\theta) = 2n_+ c \sum_{i'_\varepsilon, i'_\theta} C(i_\varepsilon, i'_\varepsilon, i_\theta, i'_\theta) n(i'_\varepsilon, i'_\theta),$$

where the bar over σ denotes averaging within the cell $(i_\varepsilon, i_\theta)$. The scattering can affect the total number of photons in the considered energy range $0.1 < \varepsilon < 10$ because scattered photons may end up outside this range. We checked that the code conserves the photon number, i.e., that the decrease of the total photon number due to scattering is equal to the photon flux through the boundary of the energy interval.

(iii) Annihilation emission

The probability that an annihilation photon has an angle within interval $(\theta, \theta + d\theta)$ is given by (see Section 3.2)

$$dP = \frac{\sin \theta d\theta}{2\gamma^2(1 - \beta \cos \theta)^2}.$$

Replacing $d\theta$ by π/N_θ and taking $\theta = (\pi/N_\theta)(i_\theta - 0.5)$, we have the probability $P(i_\theta)$ for an annihilation photon to be in cell $(i_\varepsilon^*, i_\theta)$, where i_ε^* corresponds to the photon energy $\varepsilon_{\text{ann}} = [\gamma(1 - \beta \cos \theta)]^{-1}$. The production rate of annihilation photons is then approximately given by

$$\dot{n}_{\text{ann}}(i_\varepsilon, i_\theta) = 2\dot{n}_+^{\text{ann}} P(i_\theta) \delta_{i_\varepsilon i_\varepsilon^*},$$

where $\dot{n}_+^{\text{ann}} = (3/8)(1 - \beta^2)c\sigma_T n_+^2$ is the rate of pair annihilation.

(iv) The transfer equation

The transfer equation reads

$$\frac{\partial n}{\partial t} = -\dot{n}_{\gamma\gamma} - \dot{n}_C^- + \dot{n}_C^+ + \dot{n}_{\text{ann}} - c \cos \theta \frac{\partial n}{\partial z}.$$

In the optically thin case (Sections 2.3 and 3.1), we neglect the terms \dot{n}_C^\pm and \dot{n}_{ann} , and we take into account the finite disc dimension by truncating the radiation at angles $\theta > \arctan(R/z)$. When simulating the optically thick atmosphere in Section 4.1, we account for all terms in the transfer equation and use the additional equation for e^\pm transfer,

$$\frac{\partial n_+}{\partial t} = \dot{n}_+^{\gamma\gamma} - \dot{n}_+^{\text{ann}} - c\beta \frac{\partial n_+}{\partial z},$$

where

$$\dot{n}_+^{\gamma\gamma} = \frac{1}{2} \sum_{i_\varepsilon, i_\theta} \dot{n}_{\gamma\gamma}(i_\varepsilon, i_\theta).$$

We model the atmosphere as a slab of height $R/2$ above the disc and divide it into 25 horizontal layers of equal thickness. Doubling the number of layers does not strongly affect the results. We set the boundary condition at $z = 0$ as being a power-law isotropic radiation field. The outer boundary condition at $z = R/2$ is free escape of the radiation. The main parameter of the problem is the compactness, l_1 , defined by equation (2). The other parameter is the spectral index of the primary radiation, α . To find a stationary state of the atmosphere we take an initially empty computational slab $z < R/2$ and follow the evolution of the radiation field and e^\pm plasma according to the transfer equation until a stationary state is established. The time step in the calculations equals $0.01R/c$.